Published in final edited form as:
Virology. 2013 December ; 447(0): . doi:10.1016/j.virol.2013.09.015.

Immune Targeting of PD-1^{hi} Expressing Cells During and Alter Antiretroviral Therapy in SIV-infected Rhesus Macaques

Diego A. Vargas-Inchaustegui[1], **Peng Xiao**[1,*], **Alison E. Hogg**[1,†], **Thorsten Demberg**[1], **Katherine McKinnon**[1], **David Venzon**[2], **Egidio Brocca-Cofano**[1,#], **Janet DiPasquale**[1], **Eun M. Lee**[3], **Lauren Hudacik**[3], **Ranajit Pal**[3], **Yongjun Sui**[1], **Jay A. Berzofsky**[1], **Linda Liu**[4], **Solomon Langermann**[4], and **Marjorie Robert-Guroff**[1]

[1]Vaccine Branch, National Cancer Institute, National Institutes of Health, Bethesda, MD 20892

[2]Biostatistics and Data Management Section, National Cancer Institute, National Institutes of Health, Bethesda, MD 20892

[3]Advanced Bioscience Laboratories Inc., Rockville, MD 20850

[4]Amplimmune Inc., Gaithersburg, MD 20878

Abstract

High-level T-cell expression of PD-1 during SIV infection is correlated with impaired proliferation and function. We evaluated the phenotype and distribution of T-cells and Tregs during antiretroviral therapy plus PD-1 modulation (using a B7-DC-Ig fusion protein) and post-ART. Chronically SIV-infected rhesus macaques received: 11 wk of ART (Group A); 11 wk of ART plus B7-DC-Ig (Group B); 11 wk of ART plus B7-DC-Ig, then 12 wk of B7-DC-Ig alone (Group C). Continuous B7-DC-Ig treatment (group C) decreased rebound viremia post-ART compared to pre-ART levels, associated with decreased PD-1^{hi} expressing T-cells and Tregs in PBMCs, and PD-1^{hi} Tregs in lymph nodes. It transiently decreased expression of Ki67 and $\alpha_4\beta_7$ in PBMC $CD4^+$ and $CD8^+$ Tregs for up to 8 wk post-ART and maintained Ag-specific T-cell responses at low levels. Continued immune modulation targeting PD-1^{hi} cells during and post-ART helps maintain lower viremia, keeps a favorable T-cell/Treg repertoire and modulates antigen-specific responses.

Keywords

PD-1; Treg; ART; immunomodulation; viremia

Corresponding Author: Dr. Marjorie Robert-Guroff, National Cancer Institute, National Institutes of Health, 41 Medlars Drive, Building 41, Room D804, Bethesda, MD 20892-5065., Office: +1-301-496-2114; Fax: +1-301-402-0055, guroffm@mail.nih.gov.
*Current addresses: Emory Vaccine Center at Yerkes National Primate Research Center, Atlanta, GA 30329
†Aeras, Rockville, MD 20850
#Center for Vaccine Research, University of Pittsburgh, Pittsburgh, PA 15261

Conflict of Interest

L.L and S.L. are employees of Amplimmune, Inc., which provided B7-DC-Ig and input on study design.

Introduction

T cell exhaustion, which leads to progressive loss of T cell antigen-specific function, is one of the major hurdles in the efficient treatment of chronic viral infections (1–3) and malignant neoplastic diseases (4, 5). Programmed death 1 (PD-1), an inhibitory surface co-receptor, is a member of the CD28/B7 family that is expressed on T cells, B cells and myeloid-derived cells (6, 7). There are two known ligands of PD-1: PD-L1 (B7-H1) and PD-L2 (B7-DC), which are expressed on the surface of a variety of hematopoietic (T cells, B cells, dendritic cells and macrophages) and non-hematopoietic cells (endothelial cells and fibroblasts) (8–12). Upon ligand-receptor interaction, PD-1 dampens TCR signaling, thus reducing cell proliferation and cytokine production, while favoring cell anergy and apoptosis (3, 6). PD-1 over-expression has been associated with T cell and Treg dysfunction in a variety of chronic viral infections such as HCV, HBV, HIV/SIV and LCMV (1, 13–20). Particularly in the case of HIV infection, increased PD-1 expression on antigen-specific $CD4^+$ and $CD8^+$ T cells has been associated with T cell exhaustion and disease progression (1), and has been identified as a unique marker for failing immune reconstitution in HIV patients undergoing antiretroviral therapy (ART) (21). Similarly, PD-1 expression levels have also been used as a reliable indicator of low-level HIV-1 and SIV replication (22). Although ART has decreased the morbidity and mortality associated with HIV infection globally (23), complete eradication of the viral reservoir (24, 25), as well as reduction of ART-associated side-effects, remain priorities in the development of new treatment strategies against HIV infection (26). Similarly, the identification of immunomodulatory therapies that might assist in viral reservoir eradication and improve Ag-specific immune responses is of great therapeutic interest.

Given that PD-1 over-expression has been extensively associated with T cell exhaustion, recent efforts have been directed towards improving T cell functionality during chronic viral infection and neoplastic malignancies by *in vivo* PD-1 blockade (2, 27–31). In the present study, we chose to target PD-1 by using B7-DC-Ig (Amplimmune, Inc.), a fusion protein consisting of the extracellular domain (ECD) of human B7-DC and the hinge and Fc domain of human IgG1. Murine B7-DC-Ig (ECD of murine B7-DC fused with the hinge and Fc domain of murine IgG_2a) in combination with cyclophosphamide, has been previously shown to enhance vaccine-mediated Ag-specific immune responses in a murine TC-1 tumor model. Furthermore, the enhancement of Ag-specific immune responses was due to a decrease in the number of tumor-infiltrated Tregs and to an overall decrease in PD^{hi} $CD8^+$ T cells. Importantly, murine B7-DC-Ig does not block PD-1/PD-L1 interaction or PD-1 detection by flow cytometry, and acts only on cells expressing high amounts of PD-1 on the cell surface (32). In order to test the potential PD-1 immunomodulatory properties of B7-DC-Ig in the context of SIV infection, we used chronically SIV_{mac251}-infected rhesus macaques and treated them with a triple cocktail of antiretroviral drugs with or without supplemental PD-1 immunomodulation (through the use of B7-DC-Ig). Concurrently, we also evaluated the impact of continuous PD-1 immunomodulation as a single therapeutic agent, by continuing B7-DC-Ig treatment for up to 12 wks post-ART release. Because of the well-documented effects of ART on Tregs and T-cells, throughout the study we evaluated the phenotype and distribution of both cell types in different tissue compartments and T-cell functionality. Our results suggest that prolonged *in vivo* targeting of PD-1 with B7-DC-Ig during and after ART favors lower systemic viral loads and helps maintain a favorable Treg and T cell repertoire.

Materials and Methods

Animals and sample collection

Fourteen naive and twenty-three SIV_{mac251}-positive rhesus macaques, chronically infected for 23 to 65 weeks, were housed at Advanced BioScience Laboratories, Inc. (ABL; Kensington, MD) or the NIH Animal Center (Poolesville, MD). Animals were maintained according to Institutional Animal Care and Use Committee guidelines and the NIH Guide for the Care and Use of Laboratory Animals. Fifteen of the SIV-infected macaques, recycled from previous vaccine studies (33, 34) were divided into three treatment groups (Fig. 2A) based on their previous immunization status, VL and $CD4^+$ T-cell counts. Two macaques in Groups A and B and one in Group C were Mamu A*01 positive; Group C also contained one B*08 positive macaque (Fig. 3B–D). ART composition and dosages were previously described (35). B7-DC-Ig fusion protein (Amplimmune, Inc; Gaithersburg, MD) was administered intravenously weekly at 10 mg/kg. B7-DC-Ig binding to macaque $CD3^+$ T-cells was confirmed by direct staining of PBMC with APC-conjugated B7-DC-Ig (data not shown).

Blood samples were collected by venipuncture of anesthetized animals into EDTA-treated collection tubes. Peripheral blood mononuclear cells (PBMC) were obtained using Ficoll-Paque PLUS gradients (GE Healthcare; Piscataway, NJ). Cells were washed and resuspended at 1×10^6 cells/ml in R-10 medium (RPMI 1640 containing 10% FBS, 2 mM L-glutamine, 1% non-essential amino acids, 1% sodium pyruvate and antibiotics). Lymph node (LN) biopsies were minced, passed through a 40 μm cell strainer, and lysed to remove red blood cells. Rectal biopsies were digested for 60 min on an orbital shaker in R-10 medium containing 1 mg/mL of collagenase II (Sigma; St Louis, MO). VL in plasma and rectal tissue were determined by NASBA (36).

Flow Cytometry

Anti-human fluorochrome-conjugated monoclonal antibodies (mAbs) known to cross-react with rhesus macaques and used in the present study are described in Table 1. Yellow and aqua LIVE/DEAD viability dyes (Invitrogen; Grand Island, NY) were used to exclude dead cells. For multiparametric flow cytometry analysis, PBMCs and tissue mononuclear cells were stained for specific surface molecules, fixed and permeabilized with either the Transcription Factor Staining Buffer Set (eBioscience; San Diego, CA) or with the Cytofix/Cytoperm Kit (BD Biosciences; San Jose, CA), and then stained for specific intracellular molecules. At least 500,000 singlet events (PBMCs) or 30,000 $CD3^+$ singlet events (tissue mononuclear cells) were acquired on a 4-laser LSR II SORP (BD Biosciences) and analyzed using FlowJo Software (TreeStar Inc; Ashland, OR). For all samples, gating was established using a combination of isotype and fluorescence-minus-one controls. Given that $PD\text{-}1^{hi}$ cells are enriched in the LN of SIV-infected macaques, we used LN cells to set up the flow cytometry gates that differentiate PD-1 negative, dim and high expression levels.

T cell Recall Assays

T cell recall responses were assayed by stimulating 2×10^6 PBMCs with 1 μg/mL SIV_{mac239} Gag peptide pools (complete sets of 15-mer peptides, overlapping by 11 and spanning the entire protein; NIH AIDS Research & Reference Reagent Program) for 6 h. Stimulation was performed in the presence of 10 μg/mL Brefeldin A, 2 μg/mL anti-CD49d and 0.375 μg/mL PE-Cy7 anti-CD28 (all from BD Biosciences). $CD3^+$ T cells were divided into $CD4^+$ and $CD8^+$ populations and for each, cells were further subdivided into $CD28^+$ $CD95^+$ central (CM) and $CD28^-$ $CD95^+$ effector memory (EM) cells. Percent cytokine secreting cells among each memory subset was then determined. Non-stimulated and SEB-treated (5μg/mL; Sigma) tubes were used as negative and positive controls, respectively. Non-stimulated

values were subtracted from Gag-stimulated samples to calculate Gag-specific cytokine secreting cells.

Statistical Analysis

Unless otherwise specified, all data reported were averaged from the number of macaques indicated in the figure legends. Results are shown as means ± standard errors of the mean. Data were analyzed using Prism (v5.03, GraphPad Software). A p value of ≤0.05 was considered statistically significant for each test.

Results

SIV-associated increased levels of PD-1 expression in T cells and Tregs

In order to evaluate the effect of *in vivo* targeting of the PD-1 pathway during and after ART, we first analyzed the distribution of PD-1 expressing T cells and Tregs (Fig. 1A) in peripheral blood mononuclear cells (PBMCs) and lymph nodes (LN). As previously reported (22), compared to naïve macaques, the frequency of total PD-1 expression in PBMCs of SIV-infected macaques was increased in both $CD4^+$ and $CD8^+$ T cells, without a significant increase in $CD4^+$ or $CD8^+$ Tregs (Fig. 1B). Interestingly, when evaluating LN of SIV-infected macaques, a significant increase in total PD-1 expression was observed in both T cells and Tregs when compared to naïve animals (Fig. 1C). Similar to previous reports (22), we confirmed that PD-1 is differentially expressed within $CD4^+$ and $CD8^+$ T cell subsets in naïve animals, and significantly increased in $CD4^+$ and $CD8^+$ central memory T cells of SIV-infected macaques (Fig. 1D). Given that PD-1 expression in T cells and Tregs follows a bimodal distribution (Fig. 2A), and that PD-1^{hi} cells represent an anergic population of T cells that can be directly targeted by murine B7-DC-Ig *in vivo* treatment (32), we separated dimly (PD-1^{dim}) and highly (PD-1^{hi}) PD-1-expressing T cells and Tregs in SIV-infected macaques. We initially observed that PD-1 expression in $CD4^+$ T cells and Tregs in SIV-infected macaques was significantly elevated in the PD-1^{hi} subset compared to naïve macaques, both in PBMCs (Fig. 2B) and LN (Fig. 2C). Similarly, $CD8^+$ PD-1^{hi} T cells (PBMC and LN) and Tregs (LN only) were also significantly increased (p<0.05) in SIV-infected macaques when compared to naïve animals (data not shown). Notably, PD-1^{hi} $CD4^+$ T cells and Tregs in the LN of SIV-infected macaques represented approximately 10–15% of all $CD4^+$ T cells and Tregs, a significant increase when compared to almost undetectable levels in naïve macaques (p<0.01, Fig. 2D).

Impact of ART and ART plus B7-DC-Ig treatment regimens on plasma and mucosal viral loads

In preliminary pilot studies we determined that B7-DC-Ig given alone for 4 wks did not affect plasma viral loads in chronically SIV-infected macaques (data not shown). Additionally, administration of ART in order to first decrease viremia in chronically infected macaques followed by 4 wks of B7-DC-Ig treatment alone did not impact viral loads in comparison to controls (data not shown). Therefore, we decided to study the effect of B7-DC-Ig treatment given during 11 weeks of ART, and included one group in which B7-DC-Ig was administered for an extended period of time following ART cessation. For this purpose, we divided 15 chronically SIV-infected rhesus macaques into 3 treatment groups (Groups: A, B and C, Fig. 3A). The following treatments were administered to each group: 1) Group A: 11 wks of daily ART (ART control group); Group B: 11 wks of daily ART plus weekly doses of B7-DC-Ig (ART + PD-1 modulation group); group C: 11 wks of daily ART plus weekly doses of B7-DC-Ig, followed by an additional 12 wks of B7-DC-Ig alone (continued PD-1 modulation group). Figure 3B–D shows plasma and rectal tissue viral loads for each animal for the duration of the study. In each group, one animal failed to significantly respond to ART (Fig. 3B–D, underlined codes) and was therefore not included in further

analyses. Geometric mean plasma viral loads for the remaining 4 animals per group are shown in Fig. 4A and display a significant response to ART (>90% reduction in plasma and tissue VL) over the 11 wk period of treatment in all treatment groups. Although plasma viral loads were reduced to undetectable levels in only some macaques (Fig. 3B–D), rectal tissue viral loads were undetectable after 8wk of ART in all assayed animals (Fig. 3B–D and Fig. 4B). As expected, upon ART cessation, plasma and rectal tissue viral loads rebounded in all animals (Fig. 4A–B). Interestingly, macaques in Group C which remained on B7-DC-Ig for an additional 12 wk were significantly different from macaques in Groups A and B (p=0.03 for the null hypothesis of equal changes in all 3 groups). Group C animals showed a decrease in median plasma viremia after ART release (wk 13 to 23) compared to median pre-ART levels (wk −11 to 0), whereas Groups A and B macaques did not (Fig. 4C).

Dynamics of T cell and Treg biodistribution during combined ART and in vivo PD-1 modulation

Given that during chronic SIV infection the proportional distribution and function of $CD4^+$ and $CD8^+$ T cells and Tregs are altered systemically (37, 38), and that ART treatment is capable of restoring their normal proportional distribution (39, 40), we monitored these cell populations throughout the duration of the study in PBMCs, LN and rectal tissue. During the first 8 wks of ART, we observed a significant increase in the proportion of $CD4^+$ T cells (Fig. 5A) in all tissue compartments assayed. This increase was only transient, and CD4+ T cells started to decrease proportionally upon ART termination at wk 11. Conversely, $CD8^+$ T cells transiently decreased in proportion (p<0.05, Fig. 5B) in PBMCs and LN during the first 8 wks of ART. Interestingly, while $CD4^+$ Tregs increased proportionally during the first 8 wks of ART in LN and rectal tissue, they were proportionally decreased in PBMCs (p<0.05, Fig. 5C). Furthermore, $CD8^+$ Tregs were significantly increased during the first 8 wks of ART only in LN (p<0.01, Fig. 5D). Overall, neither combined (during ART, group B) nor prolonged (during and after ART, group C) *in vivo* PD-1 modulation affected the bio-distribution of $CD4^+$ and $CD8^+$ T cells and Tregs (Fig. 5A–D).

Effect of B7-DC-Ig on PD-1^{hi} T cells and Tregs

Given that murine B7-DC-Ig affects only cells that express high amounts of surface PD-1 (32), and because high levels of PD-1 expression are observed during the chronic stage of HIV/SIV infection (2), we monitored the proportion of PD-1^{hi} T cells and Tregs during the course of this study.

Although ART transiently decreased the percentage of PD-1^{hi} expressing $CD4^+$ (Fig. 6A) and $CD8^+$ (Fig. 6B) T cells within PBMC, only animals treated with B7-DC-Ig decreased the percentage of PD-1^{hi} T cells to levels comparable to those of naïve animals (Fig. 6A, B dotted line). Moreover, continuous B7-DC-Ig treatment (Group C) maintained PD-1^{hi} T-cells at low proportions for up to 12 wks post- ART (Fig. 6A–B, wk 23). Similarly, PD-1^{hi} Tregs within PBMC were reduced in Groups B and C that received B7-DC-Ig but not by ART alone (Fig. 6C–D). Although $CD8^+$ PD-1^{hi} Tregs were maintained at low levels after ART release by continuous B7-DC-Ig treatment (Fig. 6D wks 19 and 23), $CD4^+$ PD-1^{hi} Tregs were maintained at low levels by continuous B7-DC-Ig treatment for only 2 wks upon ART release (Fig. 6C). Similarly to results in PBMC, continuous B7-DC-Ig treatment also maintained significantly lower levels of LN PD-1^{hi} $CD4^+$ and PD-1^{hi} $CD8^+$ Iregs (Fig. 6G–H), but not T cells (Fig. 6E–F).

Notably, the continuous B7-DC-Ig treatment did not elicit any toxicity. A previous GLP-compliant pharmacology and toxicology study in naïve healthy cynomolgus monkeys showed that a 10 mg/kg weekly repeated dose induced anti-drug antibodies (ADA) in only a small percentage of animals (data not shown). We did not assess ADA here, but the

extracellular domain of B7-DC is highly conserved between humans, cynomolgus monkeys and rhesus macaques (≥96% homology) and we did not expect significant antibody induction that would alter treatment outcomes. This is supported by the continuous effects of B7-DC-Ig in Group C macaques on PD-1^{hi} T cells and Tregs in PBMC and LN (Fig. 6A,B,D,G,H).

Prolonged B7-DC-Ig treatment transiently modulates Treg phenotype in SIV-infected macaques and controls the magnitude of Ag-specific T-cell responses

Increased PD-1 expression is a reliable marker of immune cell exhaustion (1, 41) and HIV/SIV viral replication and disease progression (16). Increased expression of $\alpha_4\beta_7$ (42, 43) and Ki67 (44, 45) have also been associated with HIV/SIV pathogenesis and immune dysfunction. We monitored $\alpha_4\beta_7$ and Ki67 co-expression in $CD4^+$ and $CD8^+$ T cells and Tregs during the course of the study. While no significant changes in the levels of $\alpha_4\beta_7$ and Ki67 co-expression were observed in conventional T cells, $\alpha_4\beta_7$ and Ki67 co-expression in $CD4^+$ and $CD8^+$ Tregs within PBMC and LN cells were impacted by continuous B7-DC-Ig treatment (Fig. 7A–D). Within PBMC, continuous B7-DC-Ig treatment significantly decreased $CD4^+$ $\alpha_4\beta_7$ $Ki67^+$ Tregs 2 wks post-ART release (Fig. 7A, Group C vs B, wk 13), while a transient (albeit non-significant) decrease was observed at wk 13 and 19 in $CD8^+$ $\alpha_4\beta_7$ $^+Ki67^+$ Tregs (Fig. 7B). In the LN, ART significantly decreased $\alpha_4\beta_7$ and Ki67 co-expression in $CD4^+$ and $CD8^+$ Tregs of all groups (Fig. 7C–D, wk 8). Continuous B7-DC-Ig treatment (Group C) maintained double-positive $\alpha_4\beta_7{}^+$ and $Ki67^+$ $CD4^+$ and $CD8^+$ Tregs at significantly lower levels for 2 wks post-ART release (Fig. 7C– D, Group C vs B, wk 13). Group C macaques also exhibited a slower rebound in $CD4^+$ and $CD8^+$ $\alpha 4$ β 7^+Ki67^+ Tregs following ART release at week 11. During ART, both groups exhibited low levels of these cells (Fig. 7C–D, wk 8). However the subsequent increase between wks 8 and 13 in Group B was significantly greater than that of Group C ($p = 0.029$).

As increased PD-1 expression on T-cells during the chronic phase of HIV/SIV infection leads to T-cell exhaustion (1, 3, 41) and because anti-PD-1 therapy has successfully reversed T-cell exhaustion in cancer and viral infections (15, 46–48) we examined SIV-specific functional responses of $CD4^+$ and $CD8^+$ T cells over the course of this study. We evaluated the combined Gag-specific production of IFN-γ, IL-2 and TNF-α in total memory ($CD95^+CD28^{-/+}$) $CD4^+$ and $CD8^+$ T cells. B7-DC-Ig treatment (Groups B and C) maintained Gag-specific cytokine production by total memory $CD8^+$ T cells at levels lower than those observed pre-ART for 2 weeks post-ART (Fig. 7E, wk 13). Moreover, continued B7-DC-Ig treatment (Group C) maintained lower Gag-specific cytokine responses in total memory $CD8^+$ T cells for 8 weeks post-ART (Fig. 7E, wk 19). Similar albeit not statistically significant trends were observed in Gag-specific cytokine production by total memory $CD4^+$ T cells under continuous B7-DC-Ig treatment (Fig. 7F, Group C).

Discussion

The potential use of immunomodulatory compounds during anti-HIV therapy is of great interest as a means to boost Ag-specific immune responses and to improve the anti-viral effects of ART and/or therapeutic vaccination (49–51). Although ART has been successful at increasing the life expectancy of HIV-infected individuals, the severity of ART-related side effects has prompted investigations of complementary and/or alternative therapeutic approaches that may lead to use of alternative anti-viral regimens. In this study, we investigated the immunomodulatory effects of B7-DC-Ig, during and after ART, in chronically SIV-infected rhesus macaques. We showed that continuous treatment with B7-DC-Ig caused a moderate overall decrease for up to 12 wks in the median rebound viremia after ART release when compared to median pre-ART levels. Furthermore, prolonged B7-DC-Ig treatment was associated with a decreased proportion of PD-1^{hi} expressing $CD8^+$ and

$CD4^+$ T cells and Tregs in PBMCs, and of PD-1^{hi} Tregs in lymph nodes for up to 12 wks post-ART. Similarly, prolonged B7-DC-Ig treatment transiently decreased the expression of Ki67 and $\alpha_4\beta_7$ in PBMC $CD4^+$ and $CD8^+$ Tregs for up to 8 wks post-ART and maintained Ag-specific T-cell responses at levels lower to those observed pre-ART. Our results suggest that continuous immune modulation through the PD-1 pathway using prolonged B7-DC-Ig treatment during and after ART helps maintain lower systemic VL, keeps a favorable Treg and T cell repertoire and modulates antigen-specific responses.

Despite the fact that *in vivo* PD-1 blockade has previously been reported to improve Ag-specific T cell responses during viral infection (15, 27, 46, 52–54), the immunomodulatory potential of a molecule that selectively targets PD-1^{hi} -expressing cells had not been evaluated in the context of chronic SIV infection and antiretroviral therapy. Interestingly, although plasma viral loads decreased similarly during ART in animals treated with and without B7-DC-Ig, upon ART-release, macaques that continued to receive B7-DC-Ig (group C) displayed a lower rebound post-ART plasma viral load when compared to pre-ART values (Fig. 4A and C). Similar, albeit not statistically significant results were observed in rectal tissue viral loads 2 wks post-ART (Fig. 4B, wk 13). Further, although frequencies of $CD4^+$ and $CD8^+$ T cells and Tregs fluctuated similarly across all three treatment groups (Fig. 5), $CD4^+$ and $CD8^+$ PD-1^{hi} T cells and Tregs within PBMCs maintained the lowest levels with continued B7-DC-Ig treatment post-ART release (Group C, Fig. 6). Our results are similar to observations in HBV-infected patients, where treatment with pegylated interferon led to long-lasting decreases in the percentage of circulating Tregs and levels of PD-1 expression in $CD4^+$ and $CD8^+$ T-cells in patients that responded to treatment (55). The mechanism(s) leading to the decreased frequency of PD-1^{hi} T –cells and Tregs has not been determined, but may include inhibition of proliferation of PD-1^{hi} CD4 T cells and Tregs as previously reported (32). Additionally, preliminary studies using murine B7-DC-Ig *in vitro* suggests the possibility of ADCC-mediated clearance of PD-1 over-expressing cells (Marshall, S.A. et al. manuscript in preparation).

The extent to which the absolute level of viral suppression during ART affected PD-1^{hi} T cells and Tregs upon ART release requires further study. Although the magnitude of declines were similar, plasma viral loads in Groups A and C dropped to lower levels than that of Group B after 11 weeks of treatment, although tissue viral loads became undetectable in all 3 groups (Fig. 4A–B). In view of the quick viremia rebound in all groups upon ART release (Fig. 4A), the prolonged maintenance of low level $CD4^+$ and $CD8^+$ PD-1^{hi} T cells and Tregs in Group C macaques appears unrelated to viral load rebound (Fig. 6). Similarly, the slower rebound of Group C macaques in $\alpha 4\ \beta\ 7^+$ $Ki67^+$ $CD4^+$ and $CD8^+$ Tregs in LN over weeks 8 to 13 also appears unrelated to absolute viral suppression, as all groups exhibited similar low levels of these cells during ART (Fig. 7C–D, wk 8). Several factors have been shown to influence stronger control of HIV viremia following release of patients from ART, including not only a low plasma viral load during primary infection, but also a higher CD4 count and female gender (56). While CD4 counts here were similar among macaque groups at ART initiation (Fig. 5), two of the 4 macaques in Group C were females. Further studies using larger group sizes and extended ART to bring viral loads to near undetectable levels in all animals will be needed to confirm these initial results of B7-DC-Ig treatment. (Fig. 5)

Previous studies using anti-PD-1 antibodies have shown promising results in the treatment of cancerous and viral malignancies (5, 15, 27, 28). These approaches are based on the use of anti-PD-1 antibodies, which target cells that express PD-1 both at dim and high levels. Although PD-1 has long been considered a marker for cell exhaustion, recent evidence shows that in the context of chronic SIV infection, PD-1 expression by T cells is more likely to be related to a specific differentiation or trafficking stage rather than serving by itself as a

reliable marker of immune exhaustion (57). Given that our B7-DC-Ig-mediated treatment uniquely targets PD-1^{hi} expressing cells without blocking PD-1-mediated signaling (32), our therapy targets mostly exhausted PD-1^{hi} -expressing cells, and does not eliminate all PD-1-expressing T cell subpopulations. Despite this selective targeting of exhausted PD-1^{hi}-expressing T cells and Tregs, we did not see an improvement of antigen-specific responses by CD4^{+} and CD8^{+} T cells and thus further experiments are needed to directly compare both anti-PD-1 immunomodulation approaches (PD-1 blockade and B7-CD-Ig treatment) in anti-cancer and anti-viral models.

We speculate that the lower levels of exhausted cells in Group C led to improved functional activities, resulting in a slower rate of viral rebound. A decrease in dysfunctional PD-1^{hi} Tregs could have favored better Treg functionality and better control of immune activation, therefore reducing the number of targets for SIV infection. Additionally, the decrease in PD-1^{hi} T-cells in the PBMC compartment could have provided sustained immune control of viremia following the initial reductions attributable to ART. Moreover, although the ART/B7-DC-Ig-mediated decrease of CD4^{+} PD-1^{hi} T-cells in the LN compartment was not significant (Fig. 4E), follicular helper CD4^{+}PD-1^{hi} T-cells (T_{fh}) have been recently shown to accumulate in LN and serve as SIV reservoirs during chronic infection (58–60). Thus, a B7-DC-Ig-mediated decrease in T_{fh} abundance may have contributed to the lower rebound in plasma VL observed. As the current study did not include phenotypic markers for T_{fh} cells, future studies need to further assess the impact of B7-DC-Ig on these cells. Furthermore, the SIV-mediated accumulation of PD-1^{hi} T cells in the LN (Fig. 2D) may reflect the need of a higher B7-DC-Ig dose for significantly reducing PD-1^{hi} T cells at this location.

Given that $\alpha_4\beta_7$ blockade has previously been shown to reduce plasma and tissue viral loads in SIV-infected macaques (61), we hypothesize that the reductions in plasma viral loads observed in our study might also be due to the B7-DC-Ig-induced transient decrease of $\alpha_4\beta_7^{+}$ and Ki67^{+} CD4^{+} Tregs observed in PBMCs and LN (Fig 7A and C). As Foxp3 (62) and CD25 are markers of T cell activation, and $\alpha_4\beta_7^{hi}$ memory CD4^{+} T cells are preferentially infected by SIV (42), the overall reduction of $\alpha_4\beta_7$- and Ki67-expressing CD4^{+}CD25^{+}Foxp3 cells might also reflect an overall decrease in SIV target cell availability and therefore explain the reduction in plasma viral loads observed in group C.

We initially observed that in SIV-infected rhesus macaques, the highest level of PD-1 expression (PD-1^{hi} cells) was exhibited by CD4^{+} Treg and T cells residing in the LN (Fig. 2D). Given that ART+B7-DC-Ig treatment significantly reduced the percentages of PD-1^{hi} CD4^{+} and CD8^{+} T cells and Tregs within PBMCs (Fig. 6), we expected an overall increase in the responding capacity of CD4^{+} and CD8^{+} T cells in Ag-specific recall assays. However, as mentioned above, CD4^{+} and CD8^{+} T cell Ag-specific immune responses fluctuated during ART and ART+B7-DC-Ig treatment but were maintained at levels lower than those at the start of treatment by continuous administration of B7-DC-Ig (Fig. 7E–F). Although B7-DC-Ig treatment selectively depletes “exhausted” PD-1^{hi} cells, the reduction in SIV antigenic load caused by ART presumably led to the decline observed in Ag-specific immune responses. In this regard, it has previously been reported that HIV-infected individuals receiving ART have a decrease in the magnitude and diversity of their virus-specific T cell receptor repertoire (63). Furthermore, initiation of ART has also been correlated with a decrease in the levels of HIV-specific cytotoxic responses of effector and memory CD8^{+} T cells (64, 65).

As summarized in recent reviews, the impact of Treg cells on HIV infection and disease progression is not clear (66, 67). Treg cells may be detrimental, as they suppress viral-specific immune responses. On the other hand, Treg cells can control immune activation, thereby decreasing overall pathology as well as the number of target cells available for HIV

infection. The Treg dichotomy may be best exhibited during the different phases of disease progression. As hypothesized by Holmes et al., prior to or during acute HIV infection, Treg cells may decrease viral-specific immunity while increasing the number of available target cells (68). In contrast, during the chronic phase of infection, Tregs may reduce immune activation, thereby reducing viremia and slowing T cell loss. Here, in macaques studied during the chronic phase of infection, we observed no differences in Treg cells among groups over the course of the study. However, macaques treated with continuous B7-DC-Ig exhibited prolonged maintenance of a lower level of PD-1^{hi} Tregs. Loss of these dysfunctional, exhausted cells could have provided enhanced function relative to the other groups of macaques, leading to better control of immune activation and better control of rebound viremia as we observed. Our results thus support the hypothesis of Holmes et al. (68). We expect that treatment with ART earlier in the disease course together with prolonged treatment with the B7-DC-Ig immune modulator might have more profound effects on viremia outcome and allow better discrimination of effects on immune response and disease progression.

Acknowledgments

We gratefully acknowledge the animal caretakers at Advanced BioScience Laboratories, Inc., for their expert care of our macaques and collection of serial samples. The following reagents were obtained through the NIH Nonhuman Primate Reagent Resource: Alpha-4/beta-7-APC and CD4-Qdot 655. The following reagent was obtained through the AIDS Research and Reference Reagent Program, Division of AIDS, NIAID, NIH: SIVmac239 Gag peptides, Complete Set. This research was supported by the Intramural Research Program of the NIH, National Cancer Institute.

References

1. Day CL, Kaufmann DE, Kiepiela P, Brown JA, Moodley ES, Reddy S, Mackey EW, Miller JD, Leslie AJ, DePierres C, Mncube Z, Duraiswamy J, Zhu B, Eichbaum Q, Altfeld M, Wherry EJ, Coovadia HM, Goulder PJ, Klenerman P, Ahmed R, Freeman GJ, Walker BD. PD-1 expression on HIV-specific T cells is associated with T-cell exhaustion and disease progression. Nature. 2006; 443:350–354. [PubMed: 16921384]
2. Porichis F, Kaufmann DE. Role of PD-1 in HIV pathogenesis and as target for therapy. Curr HIV/AIDS Rep. 2012; 9:81–90. [PubMed: 22198819]
3. Wherry EJ. T cell exhaustion. Nat Immunol. 2011; 12:492–499. [PubMed: 21739672]
4. Kim PS, Ahmed R. Features of responding T cells in cancer and chronic infection. Curr Opin Immunol. 2010; 22:223–230. [PubMed: 20207527]
5. Norde WJ, Hobo W, van der Voort R, Dolstra H. Coinhibitory molecules in hematologic malignancies: targets for therapeutic intervention. Blood. 2012; 120:728–736. [PubMed: 22563087]
6. Riley JL. PD-1 signaling in primary T cells. Immunol Rev. 2009; 229:114–125. [PubMed: 19426218]
7. Ishida Y, Agata Y, Shibahara K, Honjo T. Induced expression of PD-1, a novel member of the immunoglobulin gene superfamily, upon programmed cell death. Embo J. 1992; 11:3887–3895. [PubMed: 1396582]
8. Keir ME, Liang SC, Guleria I, Latchman YE, Qipo A, Albacker LA, Koulmanda M, Freeman GJ, Sayegh MH, Sharpe AH. Tissue expression of PD-L1 mediates peripheral T cell tolerance. J Exp Med. 2006; 203:883–895. [PubMed: 16606670]
9. Singh AK, Stock P, Akbari O. Role of PD-L1 and PD-L2 in allergic diseases and asthma. Allergy. 2011; 66:155–162. [PubMed: 20722638]
10. Rodriguez-Garcia M, Porichis F, de Jong OG, Levi K, Diefenbach TJ, Lifson JD, Freeman GJ, Walker BD, Kaufmann DE, Kavanagh DG. Expression of PD-L1 and PD-L2 on human macrophages is up-regulated by HIV-1 and differentially modulated by IL-10. J Leukoc Biol. 2011; 89:507–515. [PubMed: 21097698]
11. Messal N, Serriari NE, Pastor S, Nunes JA, Olive D. PD-L2 is expressed on activated human T cells and regulates their function. Mol Immunol. 2011; 48:2214–2219. [PubMed: 21752471]

12. Francisco LM, Sage PT, Sharpe AH. The PD-1 pathway in tolerance and autoimmunity. Immunol Rev. 2010; 236:219–242. [PubMed: 20636820]
13. Yao ZQ, King E, Prayther D, Yin D, Moorman J. T cell dysfunction by hepatitis C virus core protein involves PD-1/PDL-1 signaling. Viral Immunol. 2007; 20:276–287. [PubMed: 17603844]
14. Kasprowicz V, Schulze Zur Wiesch J, Kuntzen T, Nolan BE, Longworth S, Berical A, Blum J, McMahon C, Reyor LL, Elias N, Kwok WW, McGovern BG, Freeman G, Chung RT, Klenerman P, Lewis-Ximenez L, Walker BD, Allen TM, Kim AY, Lauer GM. High level of PD-1 expression on hepatitis C virus (HCV)-specific CD8+ and CD4+ T cells during acute HCV infection, irrespective of clinical outcome. J Virol. 2008; 82:3154–3160. [PubMed: 18160439]
15. Velu V, Titanji K, Zhu B, Husain S, Pladevega A, Lai L, Vanderford TH, Chennareddi L, Silvestri G, Freeman GJ, Ahmed R, Amara RR. Enhancing SIV-specific immunity in vivo by PD-1 blockade. Nature. 2009; 458:206–210. [PubMed: 19078956]
16. Petrovas C, Price DA, Mattapallil J, Ambrozak DR, Geldmacher C, Cecchinato V, Vaccari M, Tryniszewska E, Gostick E, Roederer M, Douek DC, Morgan SH, Davis SJ, Franchini G, Koup RA. SIV-specific CD8+ T cells express high levels of PD1 and cytokines but have impaired proliferative capacity in acute and chronic SIVmac251 infection. Blood. 2007; 110:928–936. [PubMed: 17440051]
17. Moorman JP, Zhang CL, Ni L, Ma CJ, Zhang Y, Wu XY, Thayer P, Islam TM, Borthwick T, Yao ZQ. Impaired hepatitis B vaccine responses during chronic hepatitis C infection: involvement of the PD-1 pathway in regulating CD4(+) T cell responses. Vaccine. 2011; 29:3169–3176. [PubMed: 21376795]
18. Jin HT, Anderson AC, Tan WG, West EE, Ha SJ, Araki K, Freeman GJ, Kuchroo VK, Ahmed R. Cooperation of Tim-3 and PD-1 in CD8 T-cell exhaustion during chronic viral infection. Proc Natl Acad Sci U S A. 2010; 107:14733–14738. [PubMed: 20679213]
19. Franceschini D, Paroli M, Francavilla V, Videtta M, Morrone S, Labbadia G, Cerino A, Mondelli MU, Barnaba V. PD-L1 negatively regulates CD4+CD25+Foxp3+ Tregs by limiting STAT-5 phosphorylation in patients chronically infected with HCV. J Clin Invest. 2009; 119:551–564. [PubMed: 19229109]
20. Shen T, Zheng J, Liang H, Xu C, Chen X, Zhang T, Xu Q, Lu F. Characteristics and PD-1 expression of peripheral CD4+CD127loCD25hiFoxP3+ Treg cells in chronic HCV infected-patients. Virol J. 2011; 8:279. [PubMed: 21645420]
21. Grabmeier-Pfistershammer K, Steinberger P, Rieger A, Leitner J, Kohrgruber N. Identification of PD-1 as a unique marker for failing immune reconstitution in HIV-1-infected patients on treatment. J Acquir Immune Defic Syndr. 2011; 56:118–124. [PubMed: 20980914]
22. Salisch NC, Kaufmann DE, Awad AS, Reeves RK, Tighe DP, Li Y, Piatak M Jr, Lifson JD, Evans DT, Pereyra F, Freeman GJ, Johnson RP. Inhibitory TCR coreceptor PD-1 is a sensitive indicator of low-level replication of SIV and HIV-1. J Immunol. 2010; 184:476–487. [PubMed: 19949078]
23. Moore RD, Keruly JC, Bartlett JG. Improvement in the health of HIV-infected persons in care: reducing disparities. Clin Infect Dis. 2012; 55:1242–1251. [PubMed: 23019271]
24. Margolis DM. Eradication therapies for HIV Infection: time to begin again. AIDS Res Hum Retroviruses. 2011; 27:347–353. [PubMed: 21314240]
25. Pace MJ, Agosto L, Graf EH, O'Doherty U. HIV reservoirs and latency models. Virology. 2011; 411:344–354. [PubMed: 21284992]
26. Calza L. Renal toxicity associated with antiretroviral therapy. HIV Clin Trials. 2012; 13:189–211. [PubMed: 22849961]
27. Nakamoto N, Kaplan DE, Coleclough J, Li Y, Valiga ME, Kaminski M, Shaked A, Olthoff K, Gostick E, Price DA, Freeman GJ, Wherry EJ, Chang KM. Functional restoration of HCV-specific CD8 T cells by PD-1 blockade is defined by PD-1 expression and compartmentalization. Gastroenterology. 2008; 134:1927–1937. [PubMed: 18549878]
28. Sakthivel P, Gereke M, Bruder D. Therapeutic intervention in cancer and chronic viral infections: antibody mediated manipulation of PD-1/PD-L1 interaction. Rev Recent Clin Trials. 2012; 7:10–23. [PubMed: 22023178]

29. Kaufmann DE, Walker BD. PD-1 and CTLA-4 inhibitory cosignaling pathways in HIV infection and the potential for therapeutic intervention. J Immunol. 2009; 182:5891–5897. [PubMed: 19414738]
30. Curiel TJ, Wei S, Dong H, Alvarez X, Cheng P, Mottram P, Krzysiek R, Knutson KL, Daniel B, Zimmermann MC, David O, Burow M, Gordon A, Dhurandhar N, Myers L, Berggren R, Hemminki A, Alvarez RD, Emilie D, Curiel DT, Chen L, Zou W. Blockade of B7-H1 improves myeloid dendritic cell-mediated antitumor immunity. Nat Med. 2003; 9:562–567. [PubMed: 12704383]
31. Mkrtichyan M, Najjar YG, Raulfs EC, Abdalla MY, Samara R, Rotem-Yehudar R, Cook L, Khleif SN. Anti-PD-1 synergizes with cyclophosphamide to induce potent anti-tumor vaccine effects through novel mechanisms. Eur J Immunol. 2011; 41:2977–2986. [PubMed: 21710477]
32. Mkrtichyan M, Najjar YG, Raulfs EC, Liu L, Langerman S, Guittard G, Ozbun L, Khleif SN. B7-DC-Ig Enhances Vaccine Effect by a Novel Mechanism Dependent on PD-1 Expression Level on T Cell Subsets. J Immunol. 2012; 189:2338–2347. [PubMed: 22837483]
33. Pegu P, Vaccari M, Gordon S, Keele BF, Doster M, Guan Y, Ferrari G, Pal R, Ferrari MG, Whitney S, Hudacik L, Billings E, Rao M, Montefiori D, Tomaras G, Alam SM, Fenizia C, Lifson JD, Stablein D, Tartaglia J, Michael N, Kim J, Venzon D, Franchini G. Antibodies with high avidity to the gp120 envelope protein in protection from SIVmac251 acquisition in an immunization regimen that mimics the RV-144 Thai Trial. J Virol. 2012; 87:1708–1719. [PubMed: 23175374]
34. Xiao P, Patterson LJ, Kuate S, Brocca-Cofano E, Thomas MA, Venzon D, Zhao J, DiPasquale J, Fenizia C, Lee EM, Kalisz I, Kalyanaraman VS, Pal R, Montefiori D, Keele BF, Robert-Guroff M. Replicating adenovirus-simian immunodeficiency virus (SIV) recombinant priming and envelope protein boosting elicits localized, mucosal IgA immunity in rhesus macaques correlated with delayed acquisition following a repeated low-dose rectal SIV(mac251) challenge. J Virol. 2012; 86:4644–4657. [PubMed: 22345466]
35. Demberg T, Brocca-Cofano E, Xiao P, Venzon D, Vargas-Inchaustegui D, Lee EM, Kalisz I, Kalyanaraman VS, Dipasquale J, McKinnon K, Robert-Guroff M. Dynamics of memory B-cell populations in blood, lymph nodes, and bone marrow during antiretroviral therapy and envelope boosting in simian immunodeficiency virus SIVmac251-infected rhesus macaques. J Virol. 2012; 86:12591–12604. [PubMed: 22973034]
36. Lee EM, Chung HK, Livesay J, Suschak J, Finke L, Hudacik L, Galmin L, Bowen B, Markham P, Cristillo A, Pal R. Molecular methods for evaluation of virological status of nonhuman primates challenged with simian immunodeficiency or simian-human immunodeficiency viruses. J Virol Methods. 2010; 163:287–294. [PubMed: 19878696]
37. Pereira LE, Villinger F, Onlamoon N, Bryan P, Cardona A, Pattanapanysat K, Mori K, Hagen S, Picker L, Ansari AA. Simian immunodeficiency virus (SIV) infection influences the level and function of regulatory T cells in SIV-infected rhesus macaques but not SIV-infected sooty mangabeys. J Virol. 2007; 81:4445–4456. [PubMed: 17314162]
38. Fauci, AS.; Desrosiers, RC. Pathogenesis of HIV and SIV. In: Coffin, JM.; Hughes, SH.; Varmus, HE., editors. Retroviruses. Cold Spring Harbor (NY); 1997.
39. Sellier P, Mannioui A, Bourry O, Dereuddre-Bosquet N, Delache B, Brochard P, Calvo J, Prevot S, Roques P. Antiretroviral treatment start-time during primary SIV(mac) infection in macaques exerts a different impact on early viral replication and dissemination. PLoS One. 2010; 5:10570.
40. Benlhassan-Chahour K, Penit C, Dioszeghy V, Vasseur F, Janvier G, Riviere Y, Dereuddre-Bosquet N, Dormont D, Le Grand R, Vaslin B. Kinetics of lymphocyte proliferation during primary immune response in macaques infected with pathogenic simian immunodeficiency virus SIVmac251: preliminary report of the effect of early antiviral therapy. J Virol. 2003; 77:12479–12493. [PubMed: 14610172]
41. Shin H, Wherry EJ. CD8 T cell dysfunction during chronic viral infection. Curr Opin Immunol. 2007; 19:408–415. [PubMed: 17656078]
42. Kader M, Wang X, Piatak M, Lifson J, Roederer M, Veazey R, Mattapallil JJ. Alpha4(+)beta7(hi)CD4(+) memory T cells harbor most Th-17 cells and are preferentially infected during acute SIV infection. Mucosal Immunol. 2009; 2:439–449. [PubMed: 19571800]

43. Kader M, Bixler S, Roederer M, Veazey R, Mattapallil JJ. CD4 T cell subsets in the mucosa are CD28+Ki-67-HLA-DR-CD69+ but show differential infection based on alpha4beta7 receptor expression during acute SIV infection. J Med Primatol. 2009; 1(38 Suppl):24–31. [PubMed: 19863675]
44. Chattopadhyay PK, Roederer M. Good cell, bad cell: flow cytometry reveals T-cell subsets important in HIV disease. Cytometry A. 2010; 77:614–622. [PubMed: 20583275]
45. Okoye A, Meier-Schellersheim M, Brenchley JM, Hagen SI, Walker JM, Rohankhedkar M, Lum R, Edgar JB, Planer SL, Legasse A, Sylwester AW, Piatak M Jr, Lifson JD, Maino VC, Sodora DL, Douek DC, Axthelm MK, Grossman Z, Picker LJ. Progressive CD4+ central memory T cell decline results in CD4+ effector memory insufficiency and overt disease in chronic SIV infection. J Exp Med. 2007; 204:2171–2185. [PubMed: 17724130]
46. Macatangay BJ, Rinaldo CR. PD-1 blockade: A promising immunotherapy for HIV? Cellscience. 2009; 5:61–65. [PubMed: 20490361]
47. Rosenblatt J, Glotzbecker B, Mills H, Vasir B, Tzachanis D, Levine JD, Joyce RM, Wellenstein K, Keefe W, Schickler M, Rotem-Yehudar R, Kufe D, Avigan D. PD-1 blockade by CT-011, anti-PD-1 antibody, enhances ex vivo T-cell responses to autologous dendritic cell/myeloma fusion vaccine. J Immunother. 2011; 34:409–418. [PubMed: 21577144]
48. Vezys V, Penaloza-MacMaster P, Barber DL, Ha SJ, Konieczny B, Freeman GJ, Mittler RS, Ahmed R. 4-1BB signaling synergizes with programmed death ligand 1 blockade to augment CD8 T cell responses during chronic viral infection. J Immunol. 2011; 187:1634–1642. [PubMed: 21742975]
49. Zajac AJ, Murali-Krishna K, Blattman JN, Ahmed R. Therapeutic vaccination against chronic viral infection: the importance of cooperation between CD4+ and CD8+ T cells. Curr Opin Immunol. 1998; 10:444–449. [PubMed: 9722921]
50. Ha SJ, Mueller SN, Wherry EJ, Barber DL, Aubert RD, Sharpe AH, Freeman GJ, Ahmed R. Enhancing therapeutic vaccination by blocking PD-1-mediated inhibitory signals during chronic infection. J Exp Med. 2008; 205:543–555. [PubMed: 18332181]
51. Finnefrock AC, Tang A, Li F, Freed DC, Feng M, Cox KS, Sykes KJ, Guare JP, Miller MD, Olsen DB, Hazuda DJ, Shiver JW, Casimiro DR, Fu TM. PD-1 blockade in rhesus macaques: impact on chronic infection and prophylactic vaccination. J Immunol. 2009; 182:980–987. [PubMed: 19124741]
52. Barber DL, Wherry EJ, Masopust D, Zhu B, Allison JP, Sharpe AH, Freeman GJ, Ahmed R. Restoring function in exhausted CD8 T cells during chronic viral infection. Nature. 2006; 439:682–687. [PubMed: 16382236]
53. Tzeng HT, Tsai HF, Liao HJ, Lin YJ, Chen L, Chen PJ, Hsu PN. PD-1 blockage reverses immune dysfunction and hepatitis B viral persistence in a mouse animal model. PLoS One. 2012; 7:e39179. [PubMed: 22761734]
54. Porichis F, Kwon DS, Zupkosky J, Tighe DP, McMullen A, Brockman MA, Pavlik DF, Rodriguez-Garcia M, Pereyra F, Freeman GJ, Kavanagh DG, Kaufmann DE. Responsiveness of HIV-specific CD4 T cells to PD-1 blockade. Blood. 2011; 118:965–974. [PubMed: 21652684]
55. Ma H, Zhang HH, Wei L. Frequency of T-cell FoxP3(+) Treg and CD4(+)/CD8(+) PD-1 expression is related to HBeAg seroconversion in hepatitis B patients on pegylated interferon. Chin Med J (Engl). 2013; 126:267–273. [PubMed: 23324275]
56. Goujard C, Girault I, Rouzioux C, Lécuroux C, Deveau C, Chaix ML, Jacomet C, Talamali A, Delfraissy JF, Venet A, Meyer L, Sinet M. and the ANRS CO6 PRIMO Study Group. 2012. HIV-1 control after transient antiretroviral treatment initiated in primary infection: role of patient characteristics and effect of therapy. Antivir Ther. 17:1001–9. [PubMed: 22865544]
57. Hong JJ, Amancha PK, Rogers K, Ansari AA, Villinger F. Re-evaluation of PD-1 expression by T cells as a marker for immune exhaustion during SIV infection. PLoS One. 2013; 8:e60186. [PubMed: 23555918]
58. Klatt NR, Vinton CL, Lynch RM, Canary LA, Ho J, Darrah PA, Estes JD, Seder RA, Moir SL, Brenchley JM. SIV infection of rhesus macaques results in dysfunctional T- and B-cell responses to neo and recall Leishmania major vaccination. Blood. 2011; 118:5803–5812. [PubMed: 21960586]

59. Perreau M, Savoye AL, De Crignis E, Corpataux JM, Cubas R, Haddad EK, De Leval L, Graziosi C, Pantaleo G. Follicular helper T cells serve as the major CD4 T cell compartment for HIV-1 infection, replication, and production. J Exp Med. 2013; 210:143–156. [PubMed: 23254284]
60. Hong JJ, Amancha PK, Rogers K, Ansari AA, Villinger F. Spatial alterations between CD4(+) T follicular helper, B, and CD8(+) T cells during simian immunodeficiency virus infection: T/B cell homeostasis, activation, and potential mechanism for viral escape. J Immunol. 2012; 188:3247–3256. [PubMed: 22387550]
61. Ansari AA, Reimann KA, Mayne AE, Takahashi Y, Stephenson ST, Wang R, Wang X, Li J, Price AA, Little DM, Zaidi M, Lyles R, Villinger F. Blocking of alpha4beta7 gut-homing integrin during acute infection leads to decreased plasma and gastrointestinal tissue viral loads in simian immunodeficiency virus-infected rhesus macaques. J Immunol. 2011; 186:1044–1059. [PubMed: 21149598]
62. Suchard MS, Mayne E, Green VA, Shalekoff S, Donninger SL, Stevens WS, Gray CM, Tiemessen CT. FOXP3 expression is upregulated in CD4T cells in progressive HIV-1 infection and is a marker of disease severity. PLoS One. 2010; 5:e11762. [PubMed: 20668701]
63. Conrad JA, Ramalingam RK, Duncan CB, Smith RM, Wei J, Barnett L, Simons BC, Lorey SL, Kalams SA. Antiretroviral therapy reduces the magnitude and T cell receptor repertoire diversity of HIV-specific T cell responses without changing T cell clonotype dominance. J Virol. 2012; 86:4213–4221. [PubMed: 22258246]
64. Casazza JP, Betts MR, Picker LJ, Koup RA. Decay kinetics of human immunodeficiency virus-specific CD8+ T cells in peripheral blood after initiation of highly active antiretroviral therapy. J Virol. 2001; 75:6508–6516. [PubMed: 11413318]
65. Kalams SA, Goulder PJ, Shea AK, Jones NG, Trocha AK, Ogg GS, Walker BD. Levels of human immunodeficiency virus type 1-specific cytotoxic T-lymphocyte effector and memory responses decline after suppression of viremia with highly active antiretroviral therapy. J Virol. 1999; 73:6721–6728. [PubMed: 10400770]
66. Moreno-Fernandez ME, Presicce P, Chougnet CA. Homeostasis and function of regulatory T cells in HIV/SIV infection. J Virol. 2012; 86:10262–10269. [PubMed: 22811537]
67. Chevalier MF, Weiss L. The split personality of regulatory T cells in HIV infection. Blood. 2013; 121:29–37. [PubMed: 23043072]
68. Holmes D, Jiang Q, Zhang L, Su L. Foxp3 and Treg cells in HIV-1 infection and immuno-pathogenesis. Immunol Res. 2008; 41:248–266. [PubMed: 18726715]

Highlights

- B7-DC-Ig modulates PD-1^{hi} cells in SIV-infected macaques during and post-ART
- Continued PD-1 modulation post-ART maintains PD-1^{hi} cells at low levels
- Continued PD-1 modulation post-ART maintains a favorable T cell and Treg repertoire

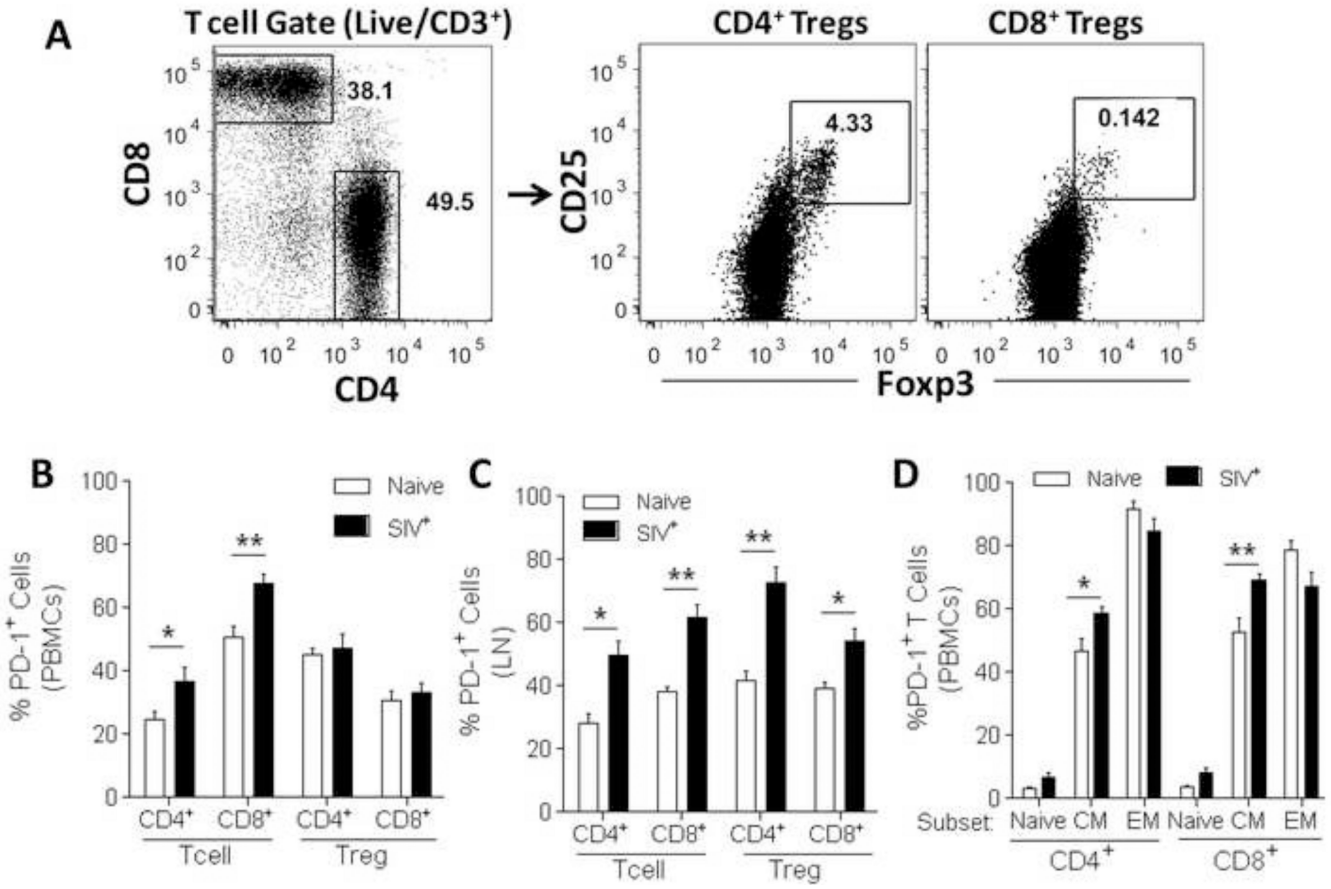

Figure 1. Increased expression of PD-1 is observed in central memory T cells as well as in CD4$^+$ and CD8$^+$ Tregs in SIV-infected rhesus macaques

Freshly isolated PBMC and LN single-cell suspensions from naïve and SIV-infected rhesus macaques were stained for analysis of PD-1 expression. (A) Gating strategy used to identify total CD4$^+$ and CD8$^+$ T cells as well as CD4$^+$ and CD8$^+$ Tregs. PD-1 expression was evaluated in CD4$^+$ and CD8$^+$ T cells and Tregs in PBMCs (B) and LN (C) cells. (D) PD-1 expression levels were analyzed in naïve (CD28$^+$ CD95$^-$), central memory (CM, CD28$^+$CD95$^+$), and effector memory (EM, CD28$^-$CD95$^+$) CD4$^+$ and CD8$^+$ T cells. PBMC data are pooled from 10 naïve and 12 SIV-infected macaques. LN data are pooled from 5 naïve and 12 SIV-infected macaques. Data are shown as means ± SEM. *, p<0.05 and **, *p*<0.01 indicate statistically significant differences between the compared groups by Mann-Whitney Test.

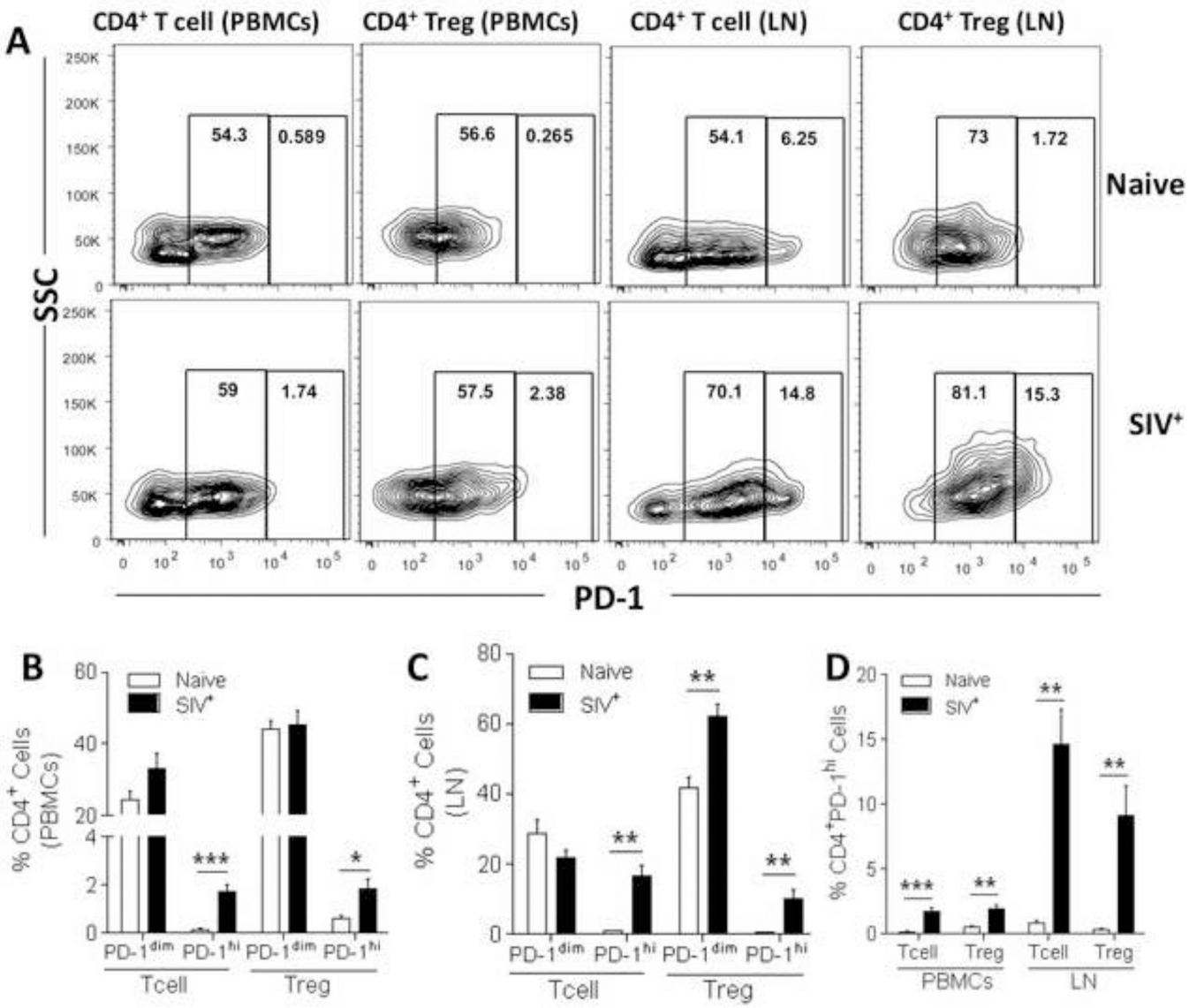

Figure 2. Proportional distribution of PD-1^{dim} and PD-1^{hi} T cells and Tregs in PBMCs and LN cells of naïve and SIV-infected macaques

(A) PD-1 positive T cells and Tregs display a bi-modal expression pattern both in PBMCs as well as in lymph nodes. (B–D) Freshly isolated PBMC and LN single-cell suspensions from naïve and SIV-infected rhesus macaques were stained for analysis of PD-1 expression. Percentages of CD4$^+$ PD-1^{dim} and PD-1^{hi} T cells and Tregs in PBMCs (B) and LN (C) cells. (D) Comparative representation of percentages of PD-1^{hi} CD4$^+$ T cells and Tregs in PBMCs and LN cells. Data are representative (A) or pooled (B–D) from at least 5 naïve and 12 SIV-infected macaques. Data are shown as means ± SEM. *, $p<0.05$, **, $p<0.01$, and ***, $p<0.001$ indicate statistically significant differences between the compared groups by Mann-Whitney Test.

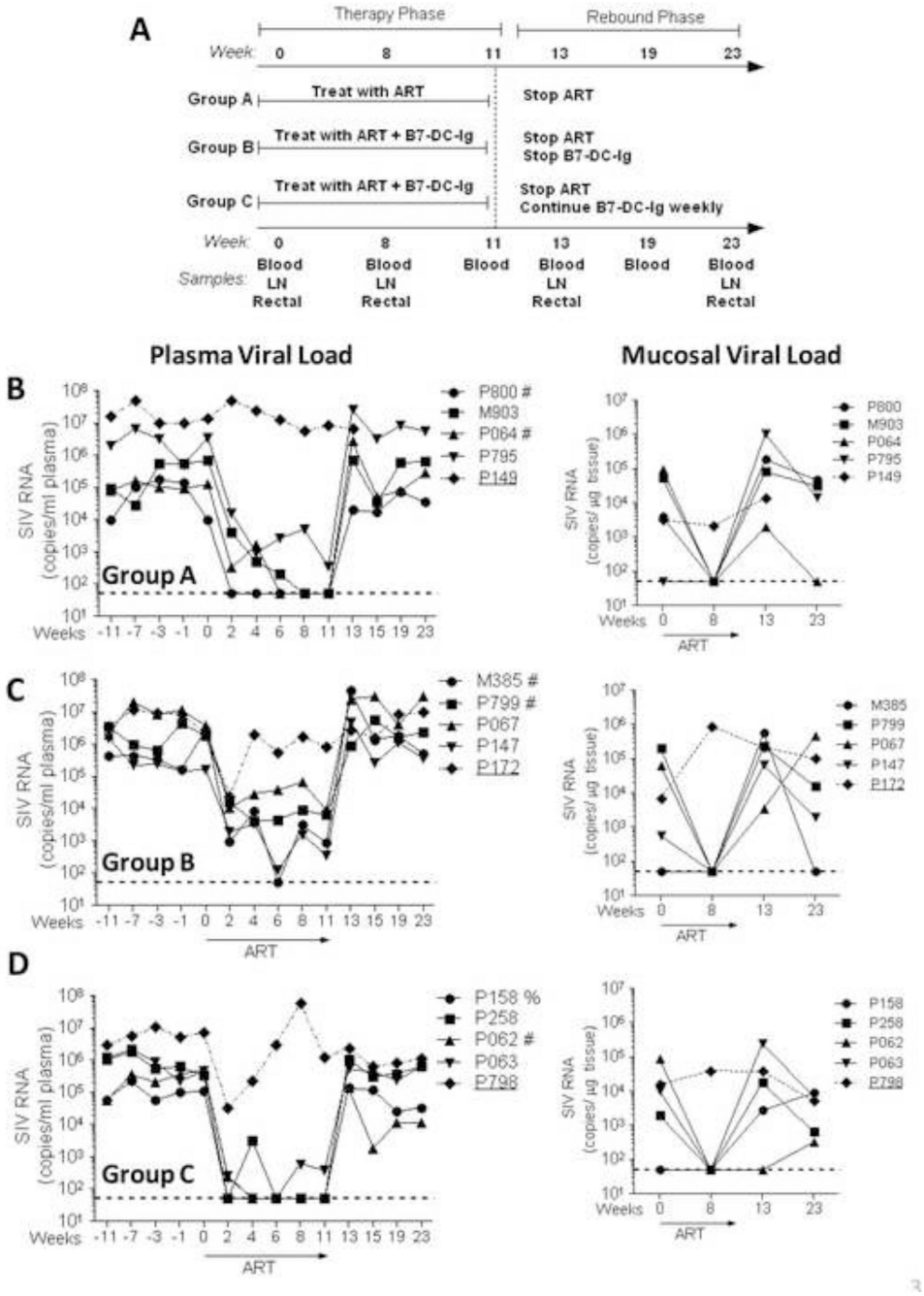

Figure 3. Therapeutic study design and plasma and rectal tissue viral loads for individual animals throughout the study

(A) Schematic description of the study design indicating the experimental groups as well as the treatment administered in each group. Time points (in weeks) for sample collection as well as type of samples collected are indicated. (B–D) Plasma and rectal tissue viral loads were obtained at the indicated time points by NASBA. Dotted lines in B–D indicate the lower limit of viremia detection (50 copies) by NASBA. Viral loads in Group A (ART-only controls) were previously reported in (35). Animals P149 (Group A), P172 (Group B) and P798 (Group C) did not respond satisfactorily to ART and were not included in further analyses. #, Mamu A*01 positive; %, Mamu B*08 positive.

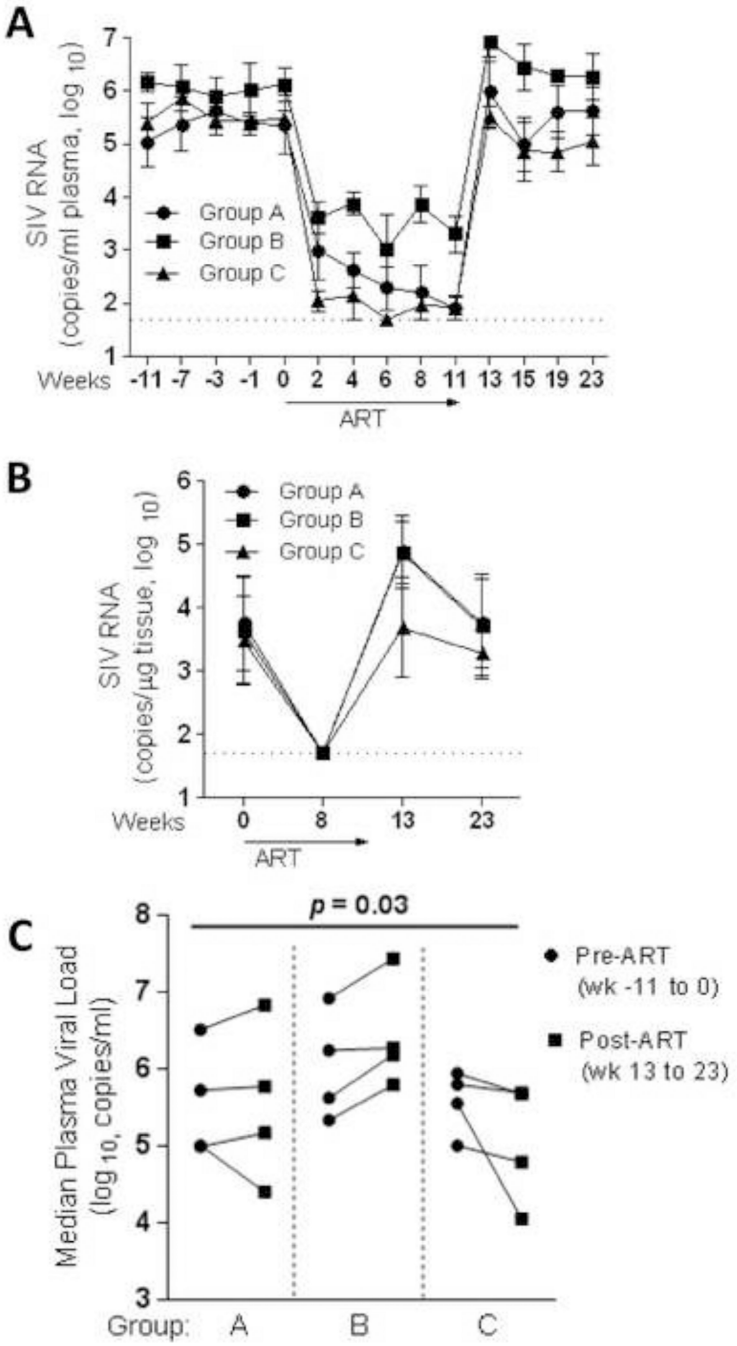

Figure 4. Impact of ART and prolonged B7-DC-Ig treatment on viral load rebound

Geometric mean plasma (A) and mucosal (B) viremia for each group was determined using the four animals per group that responded satisfactorily to ART. (C) Pre-ART vs. Post-ART median plasma viral load changes in each of the assayed groups. The changes in pre- vs post-ART median viral loads were compared across all three groups by the exact Kruskal-Wallis test.

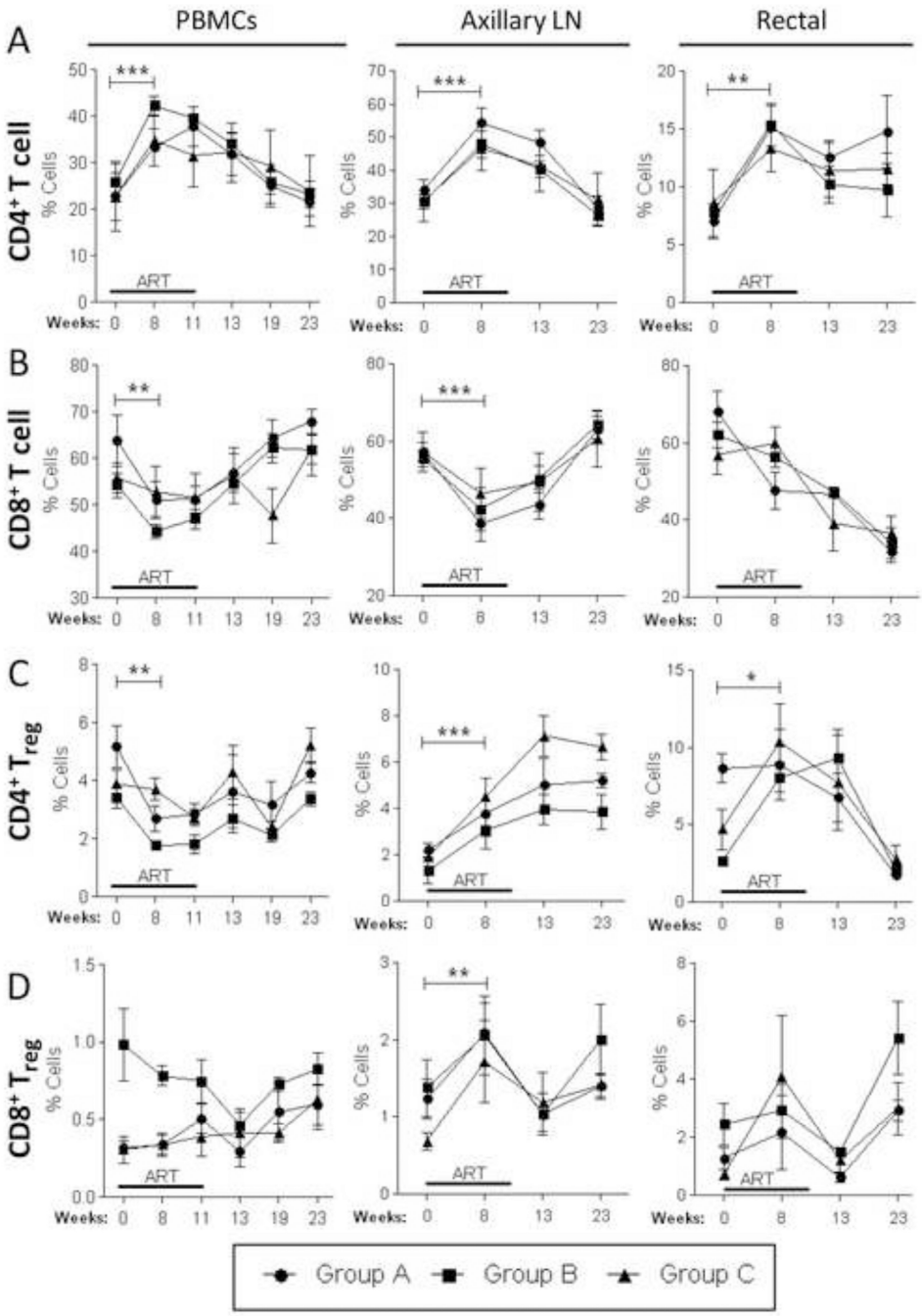

Figure 5. Proportional and compartmental distribution of CD4 and CD8 T cells and Tregs over the course of the study

Blood, LN and rectal tissue samples (*n*=4 per group) were collected at different time points as indicated in Fig. 3A and stained for flow cytometric determination of T cell and Treg percentages. Proportional counts of $CD4^+$ (A) and $CD8^+$ (B) T cells, as well as, $CD4^+$ (C) and $CD8^+$ (D) Tregs were done at each indicated time point for each tissue. Data are shown as means ± SEM. *, $p<0.05$, **, $p<0.01$, and ***, $p<0.001$ indicate statistically significant differences between the indicated time points by the Wilcoxon signed rank test.

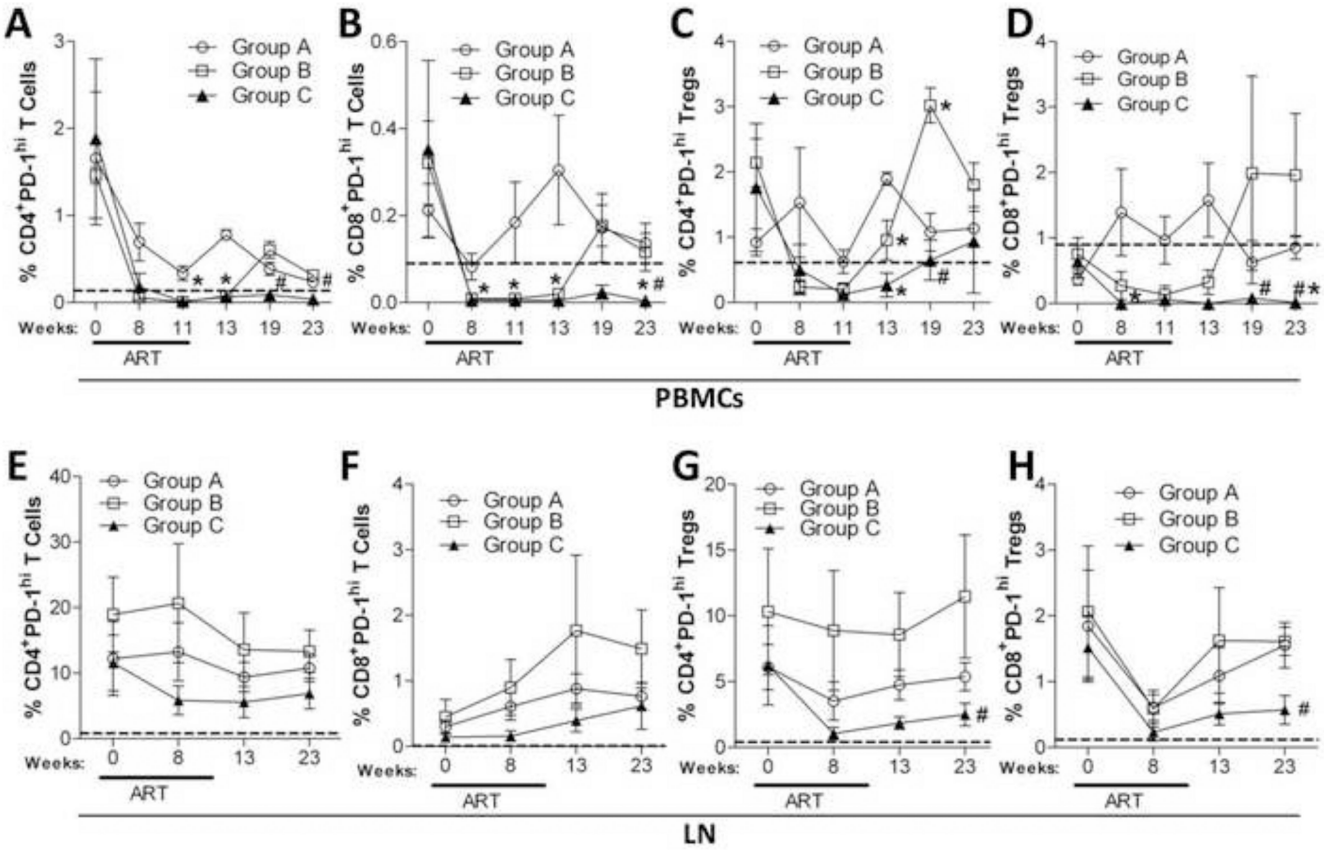

Figure 6. B7-DC-Ig treatment during and after ART significantly decreases the percentage of circulatory PD-1^{hi} CD4^{+} and CD8^{+} T cells and Tregs

PBMCs and LN cells were isolated at the indicated time points and stained for flow cytometric analysis of PD-1 expression. CD4^{+} (A and E) and CD8^{+} (B and F) PD-1^{hi} T-cells, as well as, CD4^{+} (C and G) and CD8^{+} (D and H) PD-1^{hi} Tregs were monitored for the duration of the study in PBMC (A–D) and LN (E–H). Dotted lines represent mean values of each cell population obtained from naïve macaques (10 for PBMCs and 5 for LN). Data are shown as means ± SEM. *, $p<0.05$ indicates statistically significant differences between Group A and Group B or C by the Mann-Whitney Test. $^{\#}$, $p<0.05$ indicates statistically significant differences between Group B and Group C by the Mann-Whitney Test.

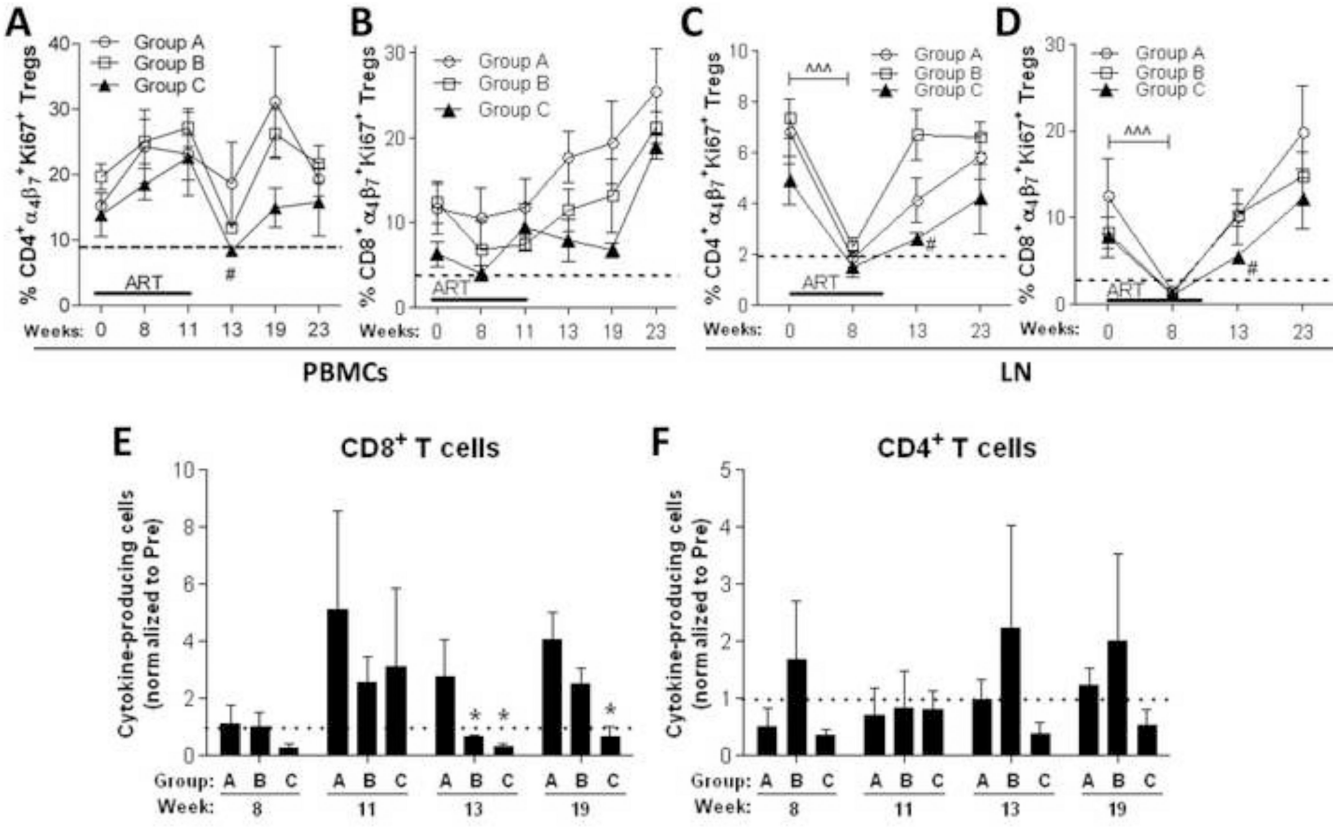

Figure 7. Prolonged B7-DC-Ig treatment transiently decreases Ki67 and $\alpha_4\beta_7$ expression in Tregs and maintains Ag-specific CD8$^+$ T-cell responses at levels lower than those observed before ART

(A–D) PBMC and LN samples were isolated at the indicated time points and stained for flow cytometric analysis of Ki67 and $\alpha_4\beta_7$ expression on CD4$^+$ and CD8$^+$ Treg cells. Co-expression of Ki67 and $\alpha_4\beta_7$ on CD4$^+$ (A) and CD8$^+$ (B) Tregs within PBMCs. (C–D) Co-expression of Ki67 and $\alpha_4\beta_7$ on CD4$^+$ (C) and CD8$^+$ (D) Tregs within LN cells. Dotted lines represent mean values of Ki67$^+\alpha_4\beta_7^+$ CD4$^+$ and CD8$^+$ Tregs as calculated from naïve macaques (10 for PBMCs and 5 for LN). (E–F) Combined Gag-specific cytokine responses (IFN-γ/TNF-α/IL-2) in total memory (CD28$^+$CD95$^{-/+}$) CD8$^+$ (E) and CD4$^+$ (F) T-cells. Data are shown as means ± SEM. In C and D, $^{\wedge\wedge\wedge}$, p<0.001 indicates statistically significant differences between the indicated time points by the Wilcoxon signed rank test. *, p<0.05 indicates statistically significant differences between Group A and Group B or C by the Mann-Whitney Test.$^{\#}p$<0.05 indicates statistically significant differences between Group B and Group C by the Mann-Whitney Test.

Table 1

Fluorochrome-conjugated monoclonal antibodies used in the present study

Antigen	Clone	Fluorochrome	Supplier
CD3	SP34-2	Alexa Fluor 700	BD Biosciences
	SP34-2	PE-Cy7	BD Biosciences
CD4	19Thy5D7	Qdot655	NIH NHPRR
	L200	Qdot605 (custom)	BD Biosciences
	OKT4	eFluor605NC	eBioscience
CD8	3B5	Qdot605	Invitrogen
	RPA-T8	eFluor650NC	eBioscience
	RPA-T8	APC-Cy7	BD Biosciences
CD25	BC96	PE-Cy7	eBioscience
CD28	CD28.2	PE-Cy7	eBioscience
	CD28.2	APC	BD Biosciences
CD95	DX2	PE-Cy5	BD Biosciences
	DX2	PE-Cy5	BioLegend
CD279 (PD-1)	eBioJ105	PE	eBioscience
Ki67	B56	FITC	BD Biosciences
Foxp3	PCH101	PerCP-Cy5.5	eBioscience
$Alpha_4Beta_7$	Rhesus recombinant	APC	NIH NHPRR
IFN-g	B27	PE	BD Biosciences
TNF-a	MAB11	PerCP-Cy5.5	BioLegend
IL-2	MQ1-17H12	APC-Cy7	BD Biosciences